01 Jan 2022

Predicting Radiated Emissions from a Complex Transportation System Wiring Harness

Fuwei Ma

Ruijie He

Sameer Walunj

Tamar Makharashvili

et. al. For a complete list of authors, see https://scholarsmine.mst.edu/ele_comeng_facwork/4688

Predicting Radiated Emissions from a Complex Transportation System Wiring Harness

Fuwei Ma, Ruijie He, Sameer Walunj, Tamar Makharashvili,
Chulsoon Hwang, Daryl Beetner
Electromagnetic Compatibility Laboratory
Missouri University of Science and Technology
Rolla, MO, USA
mafu@mst.edu, daryl@mst.edu

Brian Booth, Kerry Martin
Deere and Company
Moline, IL, USA

***Abstract*—Low frequency radiated emissions problems are often caused by common mode currents flowing on wiring harnesses. The ability to predict radiated emissions problems early in the design process can save both time and money and result in a better product. Methods have previously been reported for rapidly characterizing common-mode sources driving a harness and then using these equivalent sources to predict radiated emissions. These methods are extended in the following paper to predict radiated emissions from a complex 32-wire harness bundle connected to an engine control unit. Rapid experimental characterization of the common mode sources is enabled using an equivalent cable bundle approximation of the original harness, where wires with roughly equivalent source and load impedances are lumped together and treated as a single equivalent wire. Sources driving the equivalent bundle were found using a specialized measurement fixture. Only a few measurements are required, even if there are many wires associated with the source and they originate at different ports on the component. Full-wave models of the equivalent harness were built and along with the equivalent source were used to predict radiated emissions. This model was able to predict radiated emissions from 20-300 MHz with reasonable accuracy, with peak emissions typically predicted within about 6 dB of measurements, when using multiple different harness lengths and routings.**

Keywords—cable harness, common-mode source, engine control unit, common-mode currents, radiated emissions, measurement.

I. INTRODUCTION

An automotive component connected to a wiring harness can drive common mode currents on the harness and generate radiated emissions [1]. When the common mode currents are known, the radiated emissions can be accurately predicted [1]-[3]. While many component level tests measure these common mode currents, their values may vary dramatically if system conditions like the load impedances or harness configuration is changed [7]. The common mode currents can be predicted with substantial information about the system [4]-[6], but this level of information is often not available or is exceedingly difficult to measure.

A method was proposed in [8] to rapidly characterize the common mode sources driving a harness bundle by taking advantage of the generalized equivalent cable bundle method to reduce the number of sources that must be characterized [9],[10]. Using this technique, the wires in the harness, and by extension the sources, can be lumped together when the sources and loads are of similar impedance. As a result, the hundreds of measurements that might be required to characterize a harness containing tens of wires is reduced to only a few. The harness studied in [8] to demonstrate this proof of concept included only seven wires which could be reduced to two groups in the equivalent harness bundle, and was not representative of a modern automotive component like an engine control unit (ECU). Only the common mode currents were predicted in this study.

The work in [8] is extended in the following paper to predict the radiated emissions from a 32-wire harness bundle that can be reduced to a four-wire equivalent harness bundle. Since this bundle consists of four sources which originate from multiple ports on the ECU, a much more sophisticated measurement and simulation process is required than in the previous example. Section II introduces the equivalent common mode source model. Methods required to characterize the source are given in Section III. The simulation approach is presented in Section IV, and are compared to measurements in Section V. Conclusions are given in Section VI.

II. EQUIVALENT COMMON-MODE SOURCE MODEL

A typical configuration of an N-wire harness is shown in Fig. 1. Each circuit has its own voltage source, source impedance and load, as well as parasitic coupling between the wires and to the common mode return. This N-wire harness can be regarded as a multiconductor transmission line. Using the generalized equivalent cable bundle method an N-wire harness can be approximated with an equivalent 4-wire multiconductor transmission line at a given frequency [9]. Here, wires are grouped according to the size of their common-mode source and

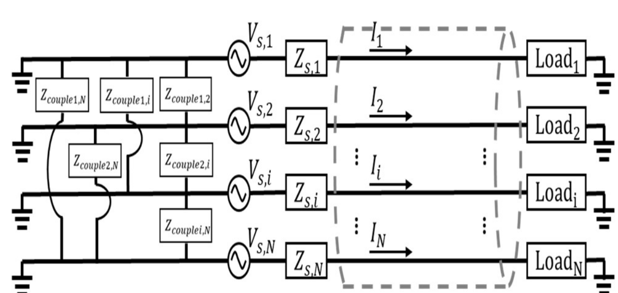

Fig. 1. Common-mode circuit describing an N-wire harness.

load impedances relative to the common mode impedance of the bundle, Z_{CM}. That is, wires with source and load impedances Z_S and Z_L are grouped together when a) $Z_S>Z_{CM}$ and $Z_L>Z_{CM}$, b) $Z_S<Z_{CM}$ and $Z_L>Z_{CM}$, c) $Z_S>Z_{CM}$ and $Z_L<Z_{CM}$, or d) $Z_S<Z_{CM}$ and $Z_L<Z_{CM}$. Only a single equivalent source and load needs to be characterized for each group, dramatically simplifying the measurement process. As a result, an equivalent common-mode source can be modeled as a four-port admittance network with four equivalent parallel current sources, as shown in Fig. 2. The four-port admittance network is described by a Y4p file which can be measured using a Vector Network Analyzer (VNA) and represents the common-mode source impedances of the modeled component. The current sources, I1-I4, are found from measurements of the source voltages at each equivalent port. The ports, S1-S4, drive the individual wires of the equivalent harness model. The equivalent harness and load can be modeled in a full-wave solver to determine the common-mode current on the harness and the resulting radiated emissions. If applying the technique over a broad frequency range, more than four equivalent sources may be required as will be explained further below.

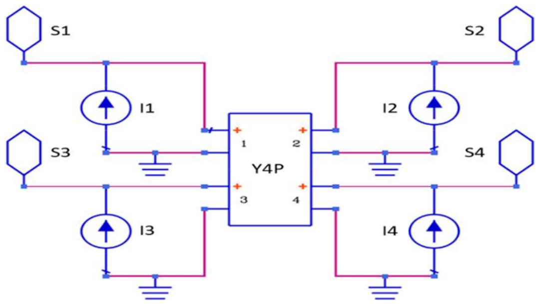

Fig. 2. Equivalent 4-port common-mode source model

III. Characterization of Common-mode Source

The system to be characterized is shown in Fig. 3 and Fig. 4. The ECU is being used to drive a harness consisting of 32 wires. The wires are each driven from one of three ports on the ECU (ECU1-ECU3). To reduce the number of equivalent sources and equivalent cable bundles, the harness was divided into groups based on the similarity of source- and load-impedances driving each wire in the 32-wire harness. In the equivalent harness bundle technique, wires are grouped according to the relative size of their source and load impedances compared to the characteristic impedance of the transmission line. In a real harness, however, the impedance of a source or load may change over frequency so that an impedance that was initially lower than the characteristic impedance at one frequency may be higher than the characteristic impedance at another or vice-versa. Since many wires in a transportation system harness will have similar types of common mode source or load impedances (e.g. load impedances that are all large resistances, or are all inductive, use that the same common-mode capacitive protection, etc.), wires were grouped here according to the similarity of the impedances seen at the two ends of the harness rather than their value relative to the characteristic impedance. This method of grouping may result in more groups than are ideally required by the equivalent harness bundle technique, but it also allows a single set of measurements and a single model to be applied over a large frequency range of interest. The 32 wires in the harness studied here were divided into four groups: the first group (called group G1) for the fourteen power wires (12V and 0V) which are connected to a Line Impedance Stabilization Network (LISN) at the far end and are assumed to be "shorted" together at high frequency at the ECU, the second group (G2) for the 7 wires connected to large resistive loads, the third group (G3) for the 5 wires connected to inductive loads around 120 nH, and the last group (G4) for wires loaded with small capacitances. The fact that the bundle could be reduced to four groups is a coincidence, and is not explicitly related to the four groups specified in the equivalent cable bundle method.

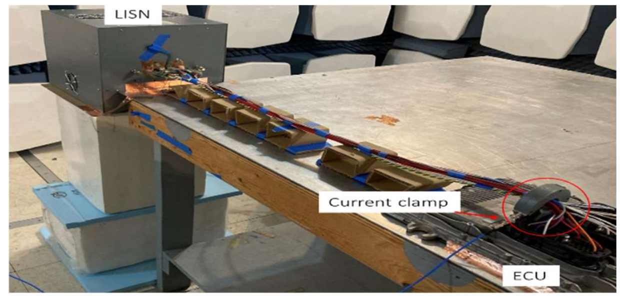

Fig. 3. The system under test consisted of an ECU connected to a 32-wire harness run over a metal ground plane.

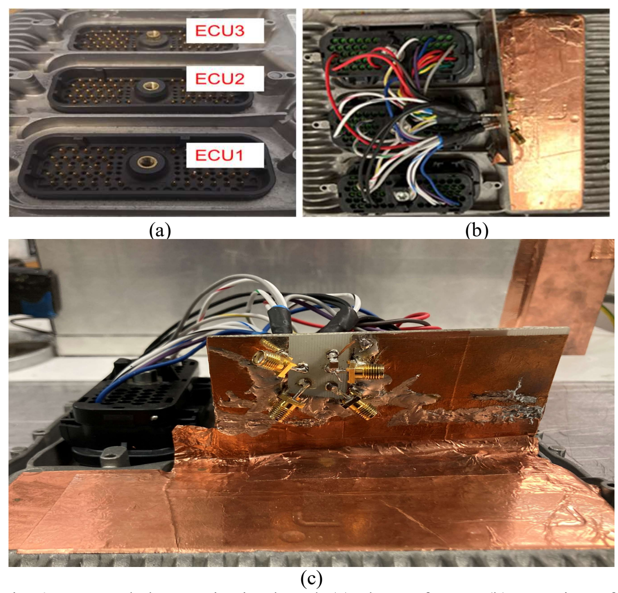

Fig. 4. ECU and characterization board. (a) Shape of ECU; (b) Top view of fixture; (c) Front view of fixture and four SMA ports.

The ECU drives the harness through three ports, (ECU1-ECU3), as shown in Fig. 4. The wires associated with each group may come from more than one of these ports, which means that a measurement fixture must be constructed which allows measurement at all three ports simultaneously. The ports are extended out from the surface of the ECU and separated by short metal ridges. Their physical configuration makes it difficult to use a single PCB or similar fixture to measure the source characteristics of each group, as was done in [8]. Such a fixture would cause unacceptable parasitics here.

To overcome this issue, the ports were characterized with respect to the voltages and currents seen at a vertical plane placed a short distance from the ports themselves, as shown in Fig. 4b and 4c. Doing so allows all the individual wires to be pulled into a harness configuration, as it would in the real application, and allows characterization of the source not at the ECU port locations but at a location where the harness begins to travel away from the ECU and into the rest of the system. Since the source characterization already includes a short portion of the harness, it should be noted that the source should be applied at the measurement plane in later simulations rather than at the ECU1-ECU3 port locations themselves. Four measurement ports are shown on the measurement plane in Fig. 4c, one for each group G1-G4. A DC block is placed between the power and signal pins and the measurement port so that measurements may be made while the ECU is powered. The measurement reference plane is electrically connected to the ECU enclosure.

Four-port VNA measurements were used to find the Y-parameter impedances associated with the four equivalent common mode sources for each group, as indicated in Fig. 5. The voltages driven by each port on the measurement plane were measured with a 4-port oscilloscope while the ECU was powered by a 12V DC battery. Using an oscilloscope allows measurement of both the magnitude and relative phase of signals at each port. The relative phase is critical for accurately determining the total common mode current on the harness. The time domain data was transformed into the frequency domain using the short-time Fourier Transform (STFT) for further analysis.

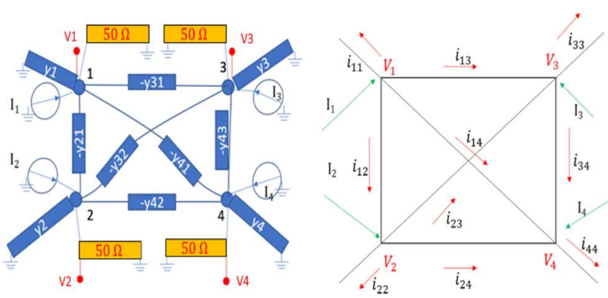

(a) (b)

Fig. 5. Characterization of source impedance. (a) Admittance network and current sources; (b) Currents at and between ports.

The voltages and impedances found at the measurement plane can be used to calculate the source currents described in Fig. 5a. The voltage at the oscilloscope is measured across the 50-ohm oscilloscope impedance in parallel with the source admittances. Including this parallel combination, the total admittance at the scope is given by:

$$\begin{aligned} Y_1 &= Y_{11} + Y_{12} + Y_{13} + Y_{14} + 0.02\ \Omega^{-1} \\ Y_2 &= Y_{21} + Y_{22} + Y_{23} + Y_{24} + 0.02\ \Omega^{-1} \\ Y_3 &= Y_{31} + Y_{32} + Y_{33} + Y_{34} + 0.02\ \Omega^{-1} \\ Y_4 &= Y_{41} + Y_{42} + Y_{43} + Y_{44} + 0.02\ \Omega^{-1} \end{aligned} \tag{1}$$

where Y_{ij} are the Y parameters describing the source impedance, as measured by the VNA, and 0.02 Ω^{-1} represents the 50 ohm oscilloscope impedance. The currents flowing in each branch of the source admittance matrix are shown in Fig. 5b. Solving at each node, the currents are related as:

$$\begin{aligned} &i_{11} = V_1 Y_1, \quad i_{22} = V_2 Y_2, \quad i_{33} = V_3 Y_3, \quad i_{44} = V_4 Y_{41}, \\ &i_{12} = (V_2 - V_1) Y_{12}, \quad i_{13} = (V_3 - V_1) Y_{13}, \\ &i_{14} = (V_4 - V_1) Y_{14}, \quad i_{23} = (V_3 - V_2) Y_{23}, \\ &i_{24} = (V_4 - V_2) Y_{24}, \quad i_{34} = (V_4 - V_3) Y_{34} \end{aligned} \tag{2}$$

where i_{ij} are given are the frequency-domain branch currents shown in Fig. 5b, and V_i is the frequency-domain voltage at each port (both magnitude and relative phase). The magnitude and phase of the source currents I_1-I_4, are then given by:

$$\begin{aligned} I_1 &= i_{11} + i_{12} + i_{13} + i_{14} \\ I_2 &= -i_{12} + i_{22} + i_{23} + i_{24} \\ I_3 &= -i_{13} - i_{23} + i_{33} + i_{34} \\ I_4 &= -i_{14} - i_{24} - i_{34} + i_{44} \end{aligned} \tag{3}$$

IV. Simulation Model

An equivalent harness bundle was created following the approach described in [9]. In this approach, each group of wires is used to create a single conductor in the equivalent harness, as shown in Fig. 6. Assuming the original harness as a uniform cross-section along its length, the 32-wire harness can be described using its per unit length RLGC matrices. The RLGC matrices for the reduced harness are found by summing self and mutual terms of the 32-wire RLGC matrices according to the grouping of the wires, as shown in [9]. The height of each equivalent conductor is given by the average height of the wires in the group. The radius of each equivalent wire is set to realize the self inductance associated with the group, and the distance between the conductors is set to realize the effective mutual inductance between the groups.

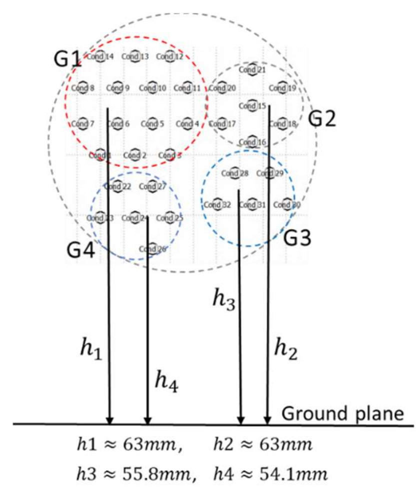

Fig. 6. Illustration of the creation of an equivalent harness bundle from the grouped wires.

Radiated emissions and common-mode currents were measured while the ECU was driving the harness as shown in Fig. 3, similar to a CISPR 25 radiated emissions test. A full wave simulation model was built in CST to predict these radiated emissions and common-mode currents as shown in Fig. 7. The harness was modeled using the four equivalent conductors as shown in Fig. 8. The harness loads were modeled in parallel as in [9]. The ECU and LISN were modelled as rectangular blocks. The wire representing the group G1 in the equivalent harness was connected to the LISN model via a 50-Ω port. In the measurement, the loads at the end of the harness were connected to the return plane through a short wire, so that the harness could maintain a consistent height along most of its length. These short wires were included in the CST model. The source at the ECU was modeled using a wave port, to account for the fact that the source is defined at a measurement plane as in Fig. 4c. A full wave model was also built of the SCHWARTZBECK VHBB 9124 4:1 BALUN biconical antenna used to measure radiated emissions in the experiments. A 200-ohm impedance was used at the antenna port to account for the antenna balun, so as to avoid modeling the balun itself.

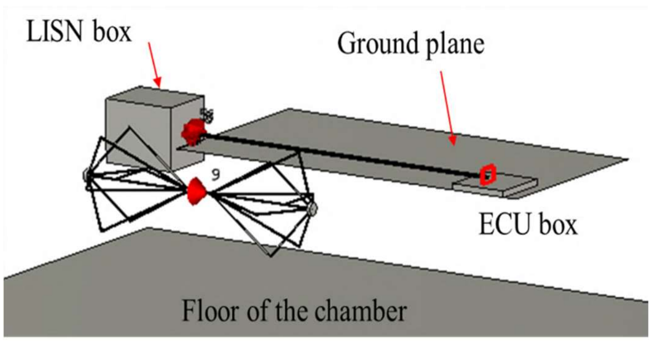

Fig. 7. CST model of the radiated emissions test setup.

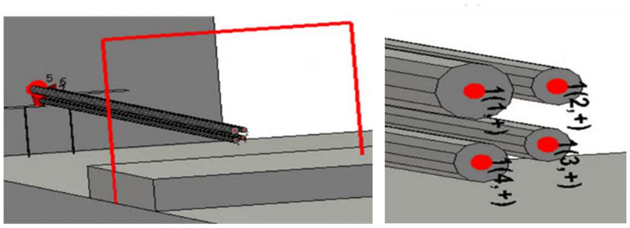

Fig. 8. Modeling of the harness bundle. (Left) Waveport driving the harness. (Right) Close up of the equivalent harness bundle.

Full-wave simulations were performed with the antenna in a vertical and horizontal polarization to find the S-parameters relating the nine simulation ports shown in Fig. 7. These S-parameters were used in a SPICE model as shown in Fig. 9 along with the ECU source model to predict the radiated emissions that would be measured from the ECU. The S parameter description of the test set up (S9P in Fig. 9) was recalculated if the harness position or length was changed.

V. Results

Fig. 10 shows a comparison of the measured and predicted common mode currents on a 1 m harness 5 cm above the return plane run straight between the ECU and LISN. The common mode currents were predicted within less than 6 dB from 20-200 MHz, confirming the accuracy of the approach. The prediction falls below the measurement above 200 MHz, where the common mode current measurements were at the noise floor of the measurement instrument.

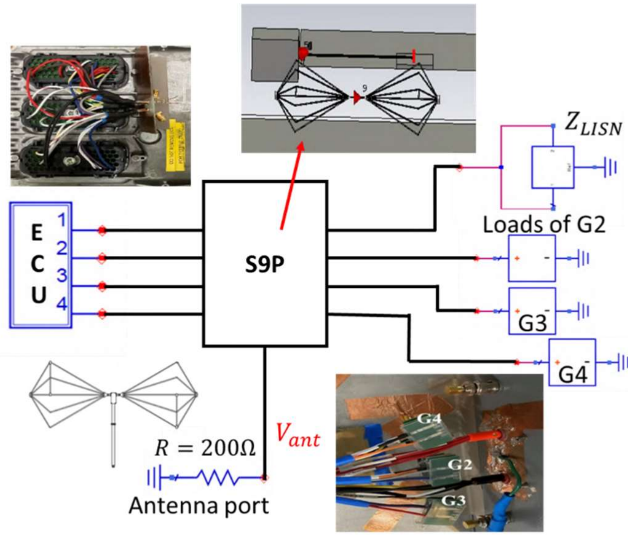

Fig. 9. Circuit model combining the source characterization of the ECU along with the full-wave model of the measurements setup in Fig. 7 used to find the radiated emissions from the system.

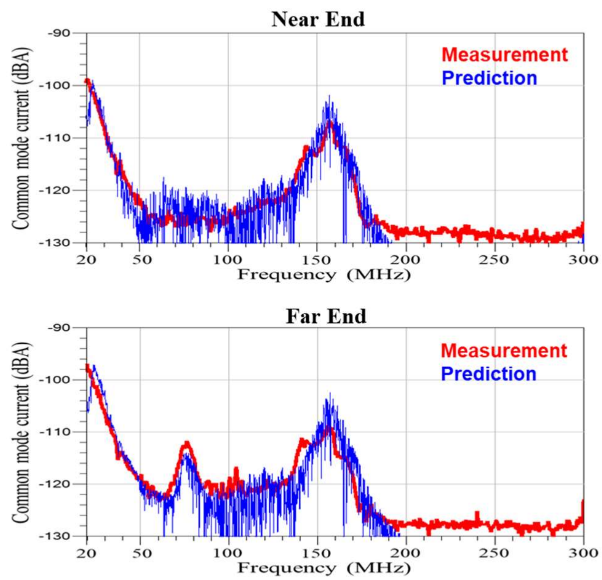

Fig. 10. Comparison of predicted and measured common mode currents on a 1-m long harness. (Top) Measured at the ECU; (Bottom) Measured at the LISN.

A comparison of the measured and simulated radiated emissions from the 1-m long harness are shown in Fig. 11. To more easily compare the prediction with the measurement, measurement "noise" was added to the estimated radiated emissions according to the following equation:

$$\mathrm{EMI} = \mathrm{dBm}\left(\frac{V_a^2}{2\times 200\,\Omega}\times \mathrm{Gain} + \mathrm{Noise}\right)$$

where Gain is the amplifier gain and noise is the noise floor of the spectrum analyzer when using a 100 kHz RBW. Predicted emissions are within and about 3 dB from 20-300 MHz.

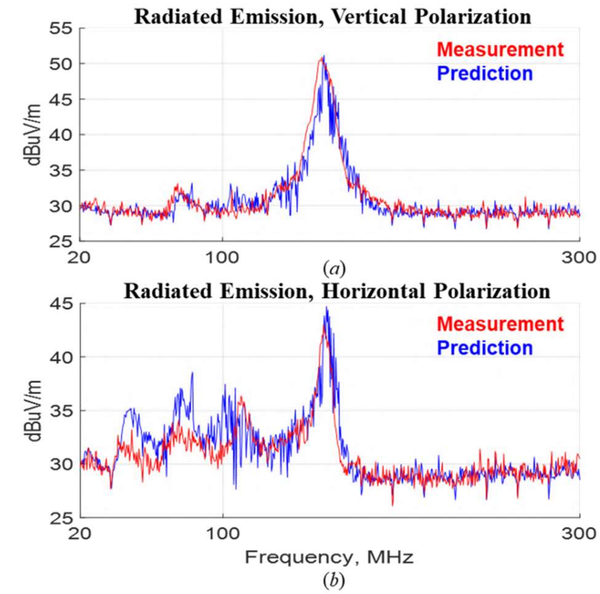

Fig. 11. Comparison of predicted and measured radiated emissions from the setup in Fig. 3 using a 1 m long harness. (Top) Vertical polarization; (Bottom) Horizontal polarization.

To further test the limits of the proposed approach, radiated emissions were studied for two additional configurations. Fig. 12 shows the radiated emissions predicted for a straight harness that is 161 cm long. While there continues to be good correlation in the trend, errors are somewhat bigger than the 1-m long case. Peaks in the measurement are still generally captured well and results are within about 6 dB, with a possible exception at roughly 180 MHz where a resonance frequency was shifted and the emissions are over-estimated.

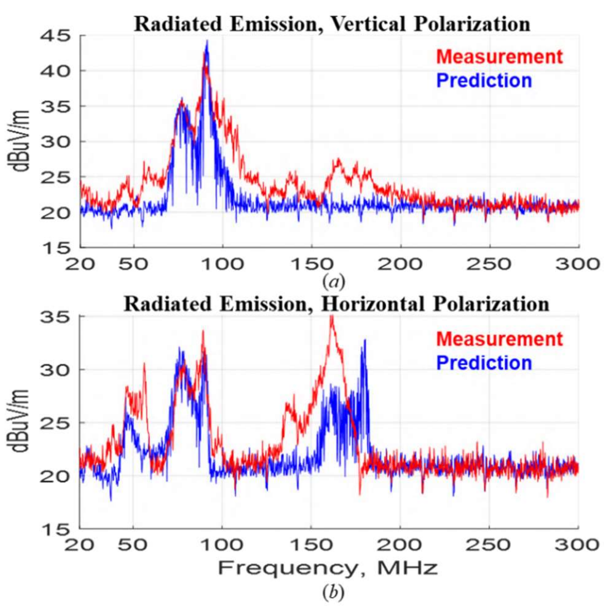

Fig. 12. Comparison of predicted and measured radiated emissions from the setup in Fig. 3 using a 161 cm long harness. (Top) Vertical polarization; (Bottom) Horizontal polarization.

Another scenario was tested where one group of wires was pulled away from the rest as shown in Fig. 13, similar to what would happen when the harness branches and connects to two different components. The length of the branch is about 27 cm, accounting for 17% of the total 161-cm harness length. The measured and predicted radiated emissions for this case are shown in Fig. 14. The emissions continue to have good correlation with the measurements.

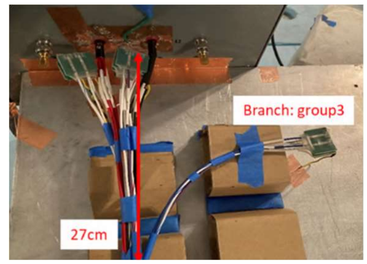

Fig. 13. Test case where one group of wires branched away from the rest.

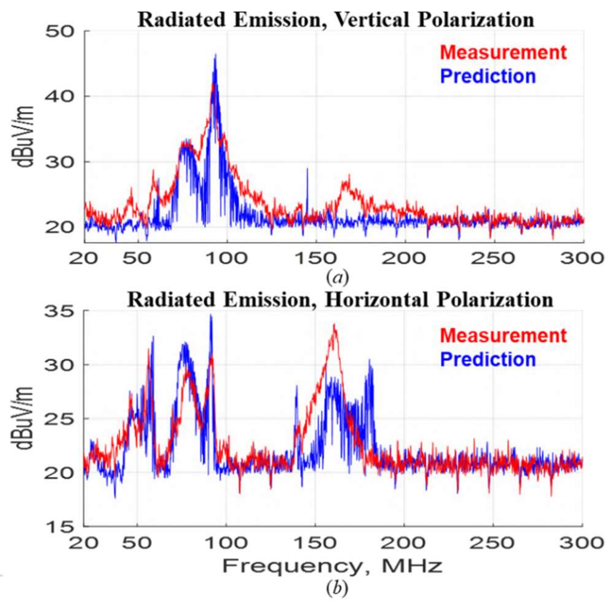

Fig. 14. Comparison of predicted and measured radiated emissions when the setup uses a 161-cm long harness with one wire group branching away from the rest. (Top) Vertical polarization; (Bottom) Horizontal polarization.

VI. Discussion and Conclusions

Methods previously developed to characterize the common mode sources associated with a component and to predict common mode currents on an equivalent two-wire harness bundle were extended here to predict radiated emissions from a more complicated harness bundle where the equivalent harness bundle contained more equivalent conductors. The extension was enabled in part by using admittance parameters to characterize the source impedances, which allows determination of multiple common mode current sources driving the harness. Wires in the original harness were grouped together when they were expected to have similar source and load impedances, so that the groupings could be used over the entire frequency range of interest. To allow accurate representation of the equivalent sources, which for a single group of wires could be driven in part from three separate ECU ports, the sources were characterized at a plane a short distance from the ECU where the wires had already come together to form the wire harness bundle. 3D simulation models driven by the equivalent component source were used to predict common mode currents and radiated emissions from the ECU connected to multiple different harness configurations. The shape of the emissions were generally predicted well and peak emissions were found within about 6 dB of those found in measurements. These results demonstrate the approach can predict emissions with good accuracy in a realistic test scenario. One challenge to predicting results was accurately representing differential mode resonances within the harness and the resulting differential-to-common mode conversion. The main advantage of this approach is that it allows relatively fast measurement of the source characteristics using only a few measurements, rather than measuring the characteristics of every wire in the bundle and the impedances between them. Simulation complexity is also improved since only a few conductors must be modeled in the equivalent harness bundle.

VII. Acknowledgment

This work was supported in part by the National Science Foundation (NSF) under Grant IIP-1916535.

References

[1] T. Makharashvili, S.Walunj, R. He, B. Booth, K. Martin, C. Hwang, D. Beetner , "Prediction of common mode current in cable harnesses," 2018 IEEE International Symposium on Electromagnetic Compatibility and 2018 IEEE Asia-Pacific Symposium on Electromagnetic Compatibility (EMC/APEMC), Singapore, 2018, pp. 321-326.

[2] D. Schneider, M. Böttcher, B. Schoch, S. Hurst, S. Tenbohlen and W. Köhler, "Transfer functions and current distribution algorithm for the calculation of radiated emissions of automotive components," 2013 International Symposium on Electromagnetic Compatibility, 2013, pp. 443-448.

[3] J. Jia, D. Rinas and S. Frei, "Predicting the Radiated Emissions of Automotive Systems According to CISPR 25 Using Current Scan Methods," in IEEE Transactions on Electromagnetic Compatibility, vol. 58, no. 2, pp. 409-418, April 2016.

[4] Geping Liu, D. J. Pommerenke, J. L. Drewniak, R. W. Kautz and Chingchi Chen, "Anticipating vehicle-level EMI using a multi-step approach," 2003 IEEE Symposium on Electromagnetic Compatibility. Symposium Record (Cat. No.03CH37446), 2003, pp. 419-424 vol.1.

[5] S. Sun, G. Liu, J. L. Drewniak and D. J. Pommerenke, "Hand-Assembled Cable Bundle Modeling for Crosstalk and Common-Mode Radiation Prediction," in IEEE Transactions on Electromagnetic Compatibility, vol. 49, no. 3, pp. 708-718, Aug. 2007.

[6] G. Li, W. Qian, A. Radchenko, J. He, G. Hess, R. Hoeckele, T. Van Doren, D. Pommerenke, D. G. Beetner, "Prediction of Radiated Emissions From Cables Over a Metal Plane Using a SPICE Model," in IEEE Transactions on Electromagnetic Compatibility, vol. 57, no. 1, pp. 61-68, Feb. 2015.

[7] R. Zamir, V. Bar-Natan and E. Recht, "System level EMC - from theory to practice," 2005 International Symposium on Electromagnetic Compatibility, Chicago, IL, pp. 741-743, Vol. 3, 2005.

[8] S. Walunj, T. Makharashvili, C. Hwang, D. Beetner, B. Booth and K. Martin, "Direct Measurement and Representation of Common-mode Sources in Cable Harnesses," 2020 IEEE International Symposium on Electromagnetic Compatibility & Signal/Power Integrity (EMCSI), 2020, pp. 118-120.

[9] G. Andrieu, L. KonÉ, F. Bocquet, B. DÉmoulin and J. Parmantier, "Multiconductor Reduction Technique for Modeling Common-Mode Currents on Cable Bundles at High Frequency for Automotive Applications," IEEE Transactions on Electromagnetic Compatibility, vol. 50, no. 1, pp. 175-184, Feb. 2008.1

[10] Z. Li, Z. J. Shao, J. Ding, Z. Y. Niu and C. Q. Gu, "Extension of the “Equivalent Cable Bundle Method” for Modeling Crosstalk of Complex Cable Bundles," IEEE Transactions on Electromagnetic Compatibility, vol. 53, no. 4, pp. 1040-1049, Nov. 2011.